Journal of Pharmacology and Toxicology

ISSN 1816-496X

Academic Journals Inc.

www.academicjournals.com

Journal of Pharmacology and Toxicology 3 (2): 64-74, 2008
ISSN 1816-496X

Molecular Modelling Analysis of the Metabolism of Terbinafine

Fazlul Huq
Discipline of Biomedical Sciences,
Faculty of Medicine, University of Sydney,
P.O. Box 170, 75 East Street, Lidcombe, NSW 1825, Australia

Abstract: Terbinafine (TBN) is an orally active allylamine derivative that has fungicidal activity against dermatocytes and many pathogenic fungi. The drug is extensively metabolized in humans with systemic clearance being dependent primarily on its biotransformation. The five most prominent metabolites found in plasma are N-desmethylterbinafine (DTBN), hydroxyterbinafine (HTBN), N-desmethylhydroxy-terbinafine (DHTBN), carboxyterbinafine (CTBN) and N-desmethylcarboxyterbinafine (DCTBN) that together account for 25% of the total urinary excretion. Four other metabolites are 1-naphthaldehyde (NAL), 1-naphthalenemethanol (NM), 1-naphthanoic acid (NA) and N-desmethylterbinafine aldehyde (DATBN). Molecular modelling analyses based on molecular mechanics, semi-empirical (PM3) and DFT (at B3LYP/6-31G* level) calculations show that TBN and its metabolites have LUMO-HOMO energy differences ranging from 4.22 to 4.73 eV based on from DFT calculations. The values suggest neither TBN nor any of its metabolites would be highly reactive or extremely inert. The molecular surface of TBN and the metabolites DATBN, NAL and DTBN are found to have significant electron-deficient regions so that they may be subject to nucleophilic attack by glutathione and nucleobases in DNA. DATBN that has been implicated as a possible cause for toxicity of TBN is found to abound most in electron-deficient regions although it has a slightly higher LUMO-HOMO energy difference than NAL. Reaction with glutathione would cause glutathione depletion resulting into oxidative stress and therefore cellular toxicity whereas the oxidation of nucleobases in DNA would cause DNA damage.

Key words: Terbinafine, antifungal agent, pathogenic, cytochrome P450, toxicity, glutathione, toxicity, molecular modelling

INTRODUCTION

Terbinafine ([(E)-N-(6,6-dimethyl-2-hepten-4-inyl)-N-methyl-1-naphthalene methenamine hydrochloride]; Lamisil; TBN) is an orally active allylamine derivative that has fungicidal activity against dermatocytes and many pathogenic fungi (Vickers *et al*., 1999). It is marketed for topical and oral use to treat dermatomycoses of skin and nails. The mechanism of action of TBN is believed to be associated with the interference of ergosterol biosynthesis through specific inhibition of lanosterol formation by blocking fungal squalene epoxidase (Ryder, 1989).

After oral administration, more than 70% of TBN is absorbed reaching its maximum plasma concentrations within 2 h (Humbert *et al*., 1998). The drug is extensively metabolized in humans with systemic clearance being dependent primarily on its biotransformation (Humbert *et al*., 1995). Fifteen different metabolites of TBN have been identified; with the major ones in human plasma

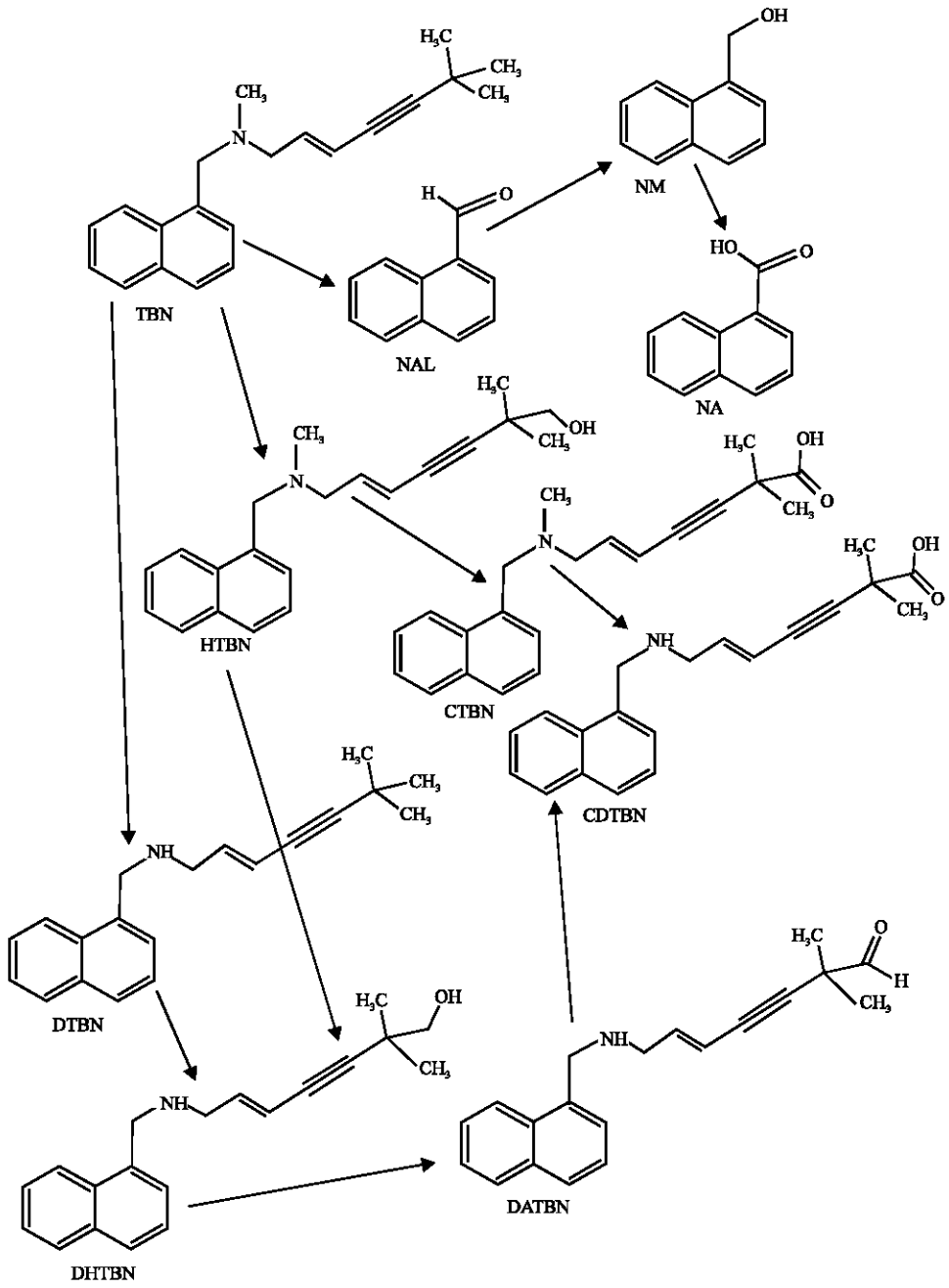

Fig. 1: Metabolic pathways for terbinafine (Vickers *et al.*, 1999)

resulting from N-demethylation, deamination, alkyl side chain oxidation and dihydrodiol formation (Vickers *et al.*, 1999). The five most prominent metabolites found in plasma are N-desmethylterbinafine (DTBN), hydroxyterbinafine (HTBN), N-desmethylhydroxyterbinafine (DHTBN), carboxyterbinafine (CTBN) and N-desmethylcarboxyterbinafine (DCTBN) that together

account for 25% of the total urinary excretion. Together with the parent drug, the five metabolites accounted for more than 80% of the total radioactivity in plasma after oral administration of ^{14}C-terbinafine. Urinary excretion accounts for more than 70% of the oral dose that contains only a trace amount of the parent drug. Four other metabolites are 1-naphthaldehyde (NAL), 1-naphthalenemethanol (NM), 1-naphthanoic acid (NA) and N-desmethylterbinafine aldehyde (DATBN).

At least seven CYP enzymes are involved in the metabolism of TBN with the most important ones being CYP2C9, CYP1A2 and CYP3A4. N-demethylation is mediated primarily by CYP2C9, CYP2C8 and CYP1A2. Dihydrodiol formation is mediated by CYP2C9 and CYP1A2 and side chain oxidation is mediated by CYP1A2, CYP2C8m CYP2c (and CYP2C19). It has been suggested that TBN may inhibit the metabolism of CYP2D6 substrates (Vickers *et al*., 1999).

Oral TBN treatment for superficial fungal infections is found to be associated with low incidence of hepatobiliary dysfunction (Iverson and Uetrecht, 2001). The metabolite DATBN has been implicated as being a possible cause for toxicity due to terbinafine. It has been suggested that this allylic aldehyde metabolite, formed in liver microsomes and conjugated with glutathione (GSH), is transported across the canalicular membrane of hepatocytes and concentrated in the bile (Iverson and Uetrecht, 2001). The mono-GSH conjugate being still reactive could bind to hepatobiliary proteins and lead to direct toxicity. Alternatively, it could modify canalicular proteins and lead to an immune-mediated reaction causing cholestatic dysfunction. It has been suggested that TBN may undergo adverse drug-drug interactions with such drugs as carbamzepine (Baath *et al*., 2006). Figure 1 summarizes the metabolic pathways of terbinafine.

In this study, molecular modelling analyses have been carried out using the program Spartan '02 (Spartan 2002) to investigate the relative stability of TBN and its metabolites with the aim of providing a better understanding of their relative toxicity.

COMPUTATIONAL METHODS

The geometries of TBN and its metabolites have been optimised based on molecular mechanics, semi-empirical and DFT calculations, using the molecular modelling program Spartan '02. Molecular mechanics calculations were carried out using MMFF force field. Semi-empirical calculations were carried out using the routine PM3. DFT calculations were carried at B3LYP/6-31G* level. In optimization calculations, a RMS gradient of 0.001 was set as the terminating condition. For the optimised structures, single point calculations were carried out to give heat of formation, enthalpy, entropy, free energy, dipole moment, solvation energy, energies for HOMO and LUMO. The order of calculations: molecular mechanics followed by semi-empirical followed by DFT ensured that the structure was not embedded in a local minimum. To further check whether the global minimum was reached, some calculations were carried out with improvable structures. It was found that when the stated order was followed, structure corresponding to the global minimum or close to that could ultimately be reached in all cases. Although RMS gradient of 0.001 may not be sufficiently low for vibrational analysis, it is believed to be sufficient for calculations associated with electronic energy levels. The study was carried out in the School of Biomedical Sciences, The University of Sydney during February to August 2006.

RESULTS AND DISCUSSION

Table 1 gives the total energy, heat of formation as per PM3 calculation, enthalpy, entropy, free energy, surface area, volume, dipole moment, energies of HOMO and LUMO as per both PM3 and DFT calculations for TBN and its metabolites NAL, NM, NA, HTBN, CTBN, DTBN, DHTBN and

DCTBN. Figure 2-10 give the regions of negative electrostatic potential (greyish-white envelopes) in (a), HOMOs (where red indicates HOMOs with high electron density) in (b), LUMOs in (c) and density of electrostatic potential (where red indicates negative, blue indicates positive and green indicates neutral) in (d), as applied to the optimised structures of TBN and its metabolites NAL, NM, NA, HTBN, CTBN, DTBN, DHTBN and DCTBN.

TBN and its metabolites are found to differ in their LUMO-HOMO energy differences (ranging from 4.28 to 5.19 eV from DFT calculations), indicating that the compounds would differ in their kinetic lability. The values suggest that none of the compounds would be extremely inert or highly labile.

Table 1: Calculated thermodynamic and other parameters of terbinafine and its metabolites

	Calculation type	Total energy (kcal mol^{-1}/ atomic unit*)	Heat of formation (kcal mol^{-1})	Enthalpy (kcal mol^{-1} K^{-1})	Entropy (cal mol^{-1} K^{-1})	Solvation energy (kcal mol^{-1} K^{-1})	Free energy (kcalmol^{-1})
TBN	PM3	78.20	79.76	266.26	159.19	-1.56	218.80
	DFT	-869.97		267.45	159.04	-1.31	220.06
NAL	PM3	2.33	7.57	104.18	92.40	-5.24	76.64
	DFT	-299.22		104.28	93.04	-4.42	76.54
NM	PM3	-11.80	-4.22	118.83	96.50	-7.59	90.05
	DFT	-500.40		119.37	95.22	-6.93	90.98
NA	PM3	-51.82	-45.53	108.15	98.18	-6.29	78.88
	DFT	-574.47		108.30	97.82	-6.04	79.13
HTBN	PM3	33.80	40.32	269.92	163.29	-6.52	221.23
	DFT	-945.18		270.78	162.65	-6.25	222.23
TBN	PM3	-8.88	1.48	259.36	167.65	-10.36	209.37
	DFT	-1019.22		260.59	166.86	-9.13	210.87
DTBN	PM3	77.50	81.71	248.49	153.11	-4.22	202.84
	DFT	-830.66		249.67	152.76	-4.01	204.15
DHTBN	PM3	33.11	42.29	252.17	157.22	-9.18	205.30
	DFT	-905.87		253.44	156.51	-8.06	206.80
DATBN	PM3	51.86	56.02	254.76	164.24	-4.15	205.79
	DFT	-943.97		255.99	163.31	-3.79	207.32
DCTBN	PM3	-8.47	3.02	241.45	162.78	-11.50	192.91
	DFT	-979.91		242.80	161.88	-10.05	195.56

Molecule	Calculation type	Area ($Å^2$)	Volume ($Å^3$)	Dipole moment (debye)	HOMO (eV)	LUMO (eV)	LUMO-HOMO (eV)
TBN	PM3	374.60	351.78	0.8	-8.77	-0.46	8.31
	DFT	375.17	352.63	0.6	-5.66	-0.95	4.71
NAL	PM3	181.57	170.65	2.9	-9.15	-0.95	8.20
	DFT	182.42	171.29	3.6	-6.21	-1.99	4.22
NM	PM3	187.67	175.24	1.4	-8.86	-0.43	8.43
	DFT	188.24	175.77	1.6	-5.67	-0.93	4.74
NA	PM3	188.63	177.17	2.0	-9.08	-0.96	8.12
	DFT	189.16	177.83	1.8	-6.07	-1.74	4.33
HTBN	PM3	381.68	358.88	1.9	-8.81	-0.49	8.32
	DFT	383.47	360.04	1.7	-5.69	-0.97	4.72
TBN	PM3	384.47	361.30	4.7	-8.88	-0.56	8.32
	DFT	383.89	361.55	5.2	-5.82	-1.17	4.65
DTBN	PM3	357.16	332.62	0.9	-8.76	-0.45	8.31
	DFT	358.22	334.10	1.1	-5.63	-0.91	4.72
DHTBN	PM3	364.18	339.71	1.5	-8.80	-0.49	8.31
	DFT	366.68	341.55	0.5	-5.66	-0.93	4.73
DATBN	PM3	377.47	354.62	2.7	-8.84	-0.53	8.31
	DFT	377.84	355.32	2.6	-5.75	-1.12	4.63
DCTBN	PM3	366.82	341.96	5.2	-8.91	-0.59	8.32
	DFT	366.76	342.98	4.9	-5.79	-1.13	4.66

*: In atomic units from DFT calculations

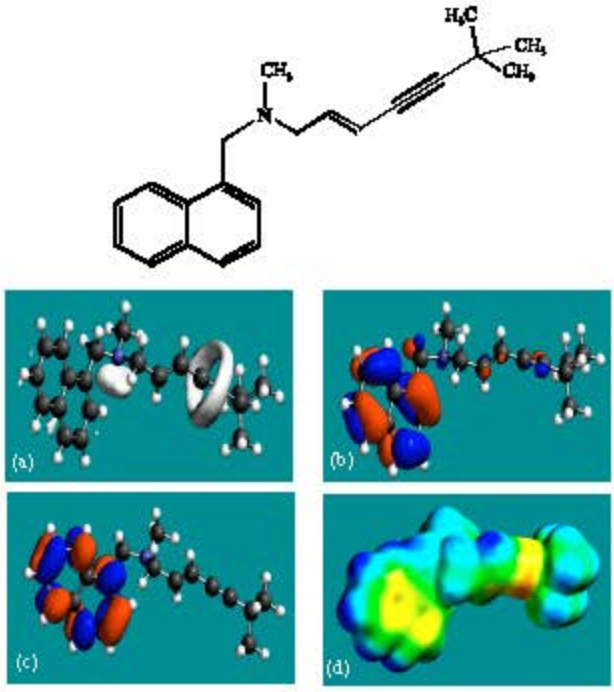

Fig. 2: Structure of TBN giving in: (a) the electrostatic potential (greyish envelope denotes negative electrostatic potential), (b) the HOMOs, (where red indicates HOMOs with high electron density), (c) the LUMOs (where blue indicates LUMOs) and in (d) density of electrostatic potential on the molecular surface (where red indicates negative, blue indicates positive and green indicates neutral)

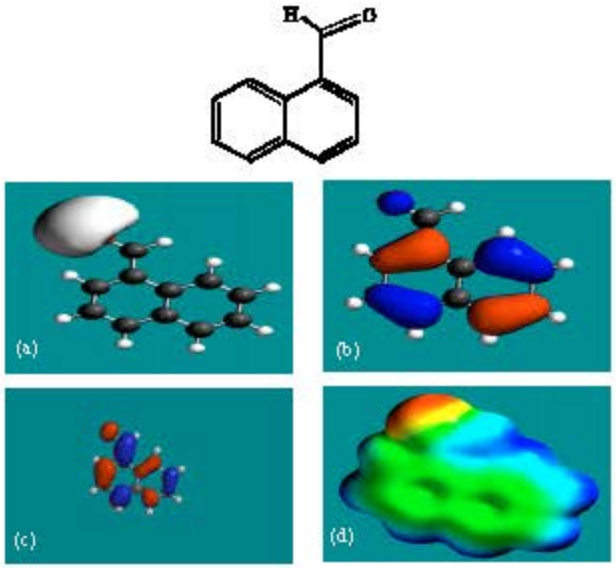

Fig. 3: Structure of NAL giving in: (a) the electrostatic potential (greyish envelope denotes negative electrostatic potential), (b) the HOMOs, (where red indicates HOMOs with high electron density), (c) the LUMOs (where blue indicates LUMOs) and in (d) density of electrostatic potential on the molecular surface (where red indicates negative, blue indicates positive and green indicates neutral)

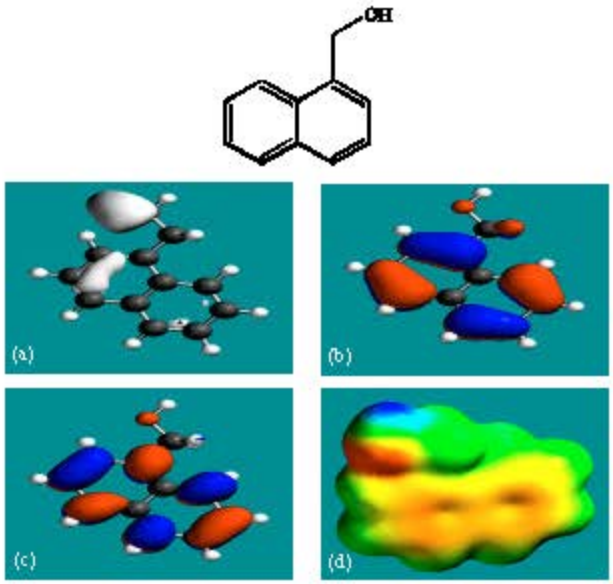

Fig. 4: Structure of NM giving in: (a) the electrostatic potential (greyish envelope denotes negative electrostatic potential), (b) the HOMOs, (where red indicates HOMOs with high electron density), (c) the LUMOs (where blue indicates LUMOs) and in (d) density of electrostatic potential on the molecular surface (where red indicates negative, blue indicates positive and green indicates neutral)

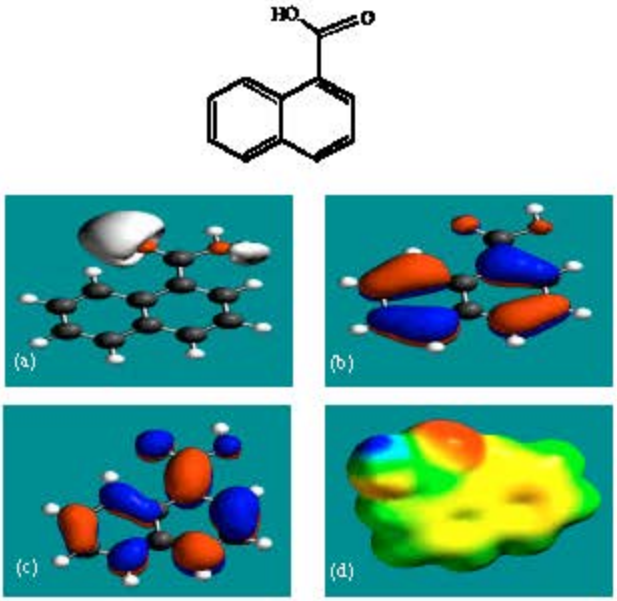

Fig. 5: Structure of NA giving in: (a) the electrostatic potential (greyish envelope denotes negative electrostatic potential), (b) the HOMOs, (where red indicates HOMOs with high electron density), (c) the LUMOs (where blue indicates LUMOs) and in (d) density of electrostatic potential on the molecular surface (where red indicates negative, blue indicates positive and green indicates neutral)

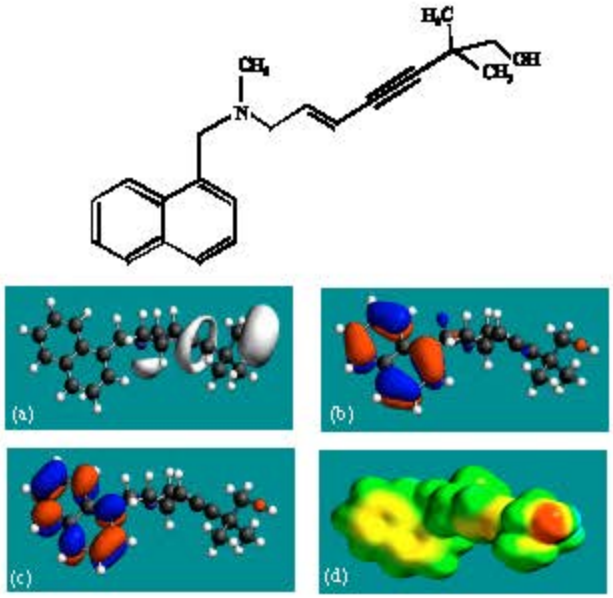

Fig. 6: Structure of HTBN giving in: (a) the electrostatic potential (greyish envelope denotes negative electrostatic potential), (b) the HOMOs, (where red indicates HOMOs with high electron density), (c) the LUMOs (where blue indicates LUMOs) and in (d) density of electrostatic potential on the molecular surface (where red indicates negative, blue indicates positive and green indicates neutral)

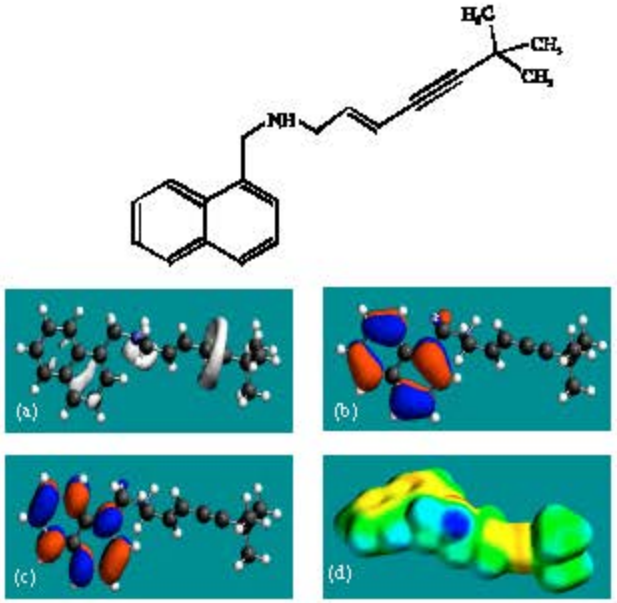

Fig. 7: Structure of DTBN giving in: (a) the electrostatic potential (greyish envelope denotes negative electrostatic potential), (b) the HOMOs, (where red indicates HOMOs with high electron density), (c) the LUMOs (where blue indicates LUMOs) and in (d) density of electrostatic potential on the molecular surface (where red indicates negative, blue indicates positive and green indicates neutral)

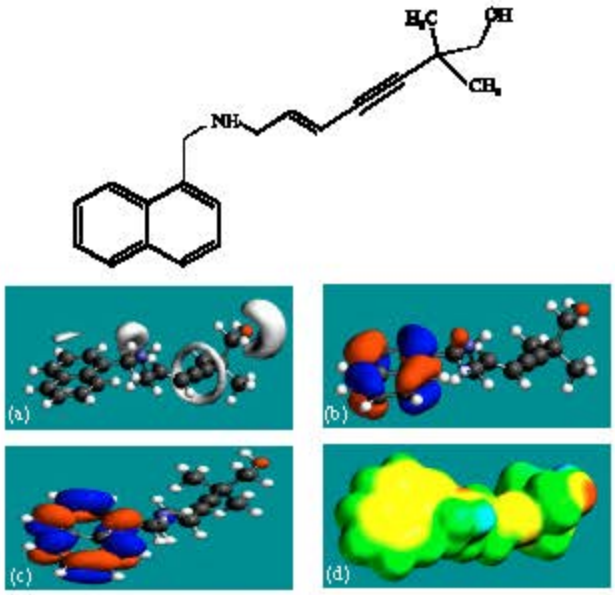

Fig. 8: Structure of DHTBN giving in: (a) the electrostatic potential (greyish envelope denotes negative electrostatic potential), (b) the HOMOs, (where red indicates HOMOs with high electron density) (c) the LUMOs (where blue indicates LUMOs) and in (d) density of electrostatic potential on the molecular surface (where red indicates negative, blue indicates positive and green indicates neutral)

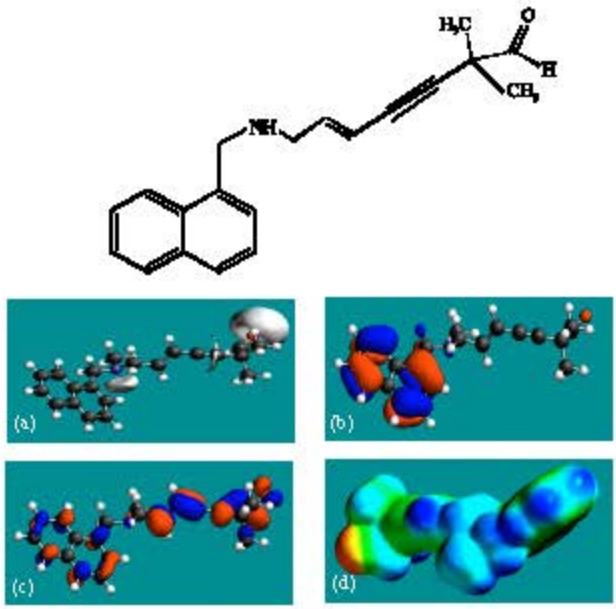

Fig. 9: Structure of DATBN giving in: (a) the electrostatic potential (greyish envelope denotes negative electrostatic potential), (b) the HOMOs, (where red indicates HOMOs with high electron density) (c) the LUMOs (where blue indicates LUMOs) and in (d) density of electrostatic potential on the molecular surface (where red indicates negative, blue indicates positive and green indicates neutral)

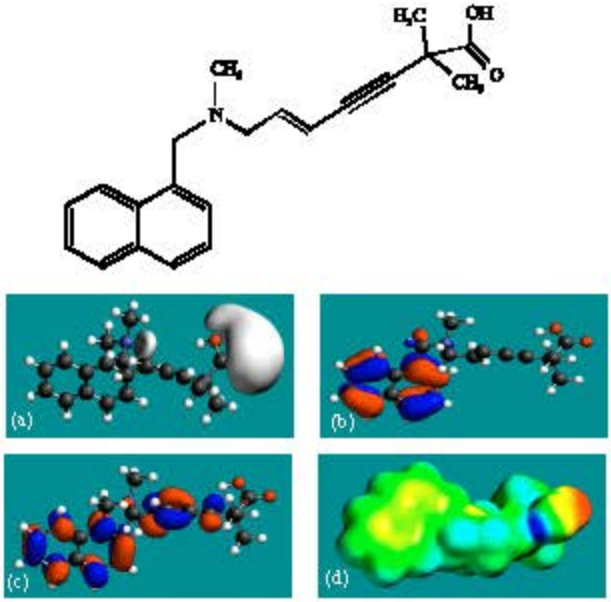

Fig. 10: Structure of CTBN giving in: (a) the electrostatic potential (greyish envelope denotes negative electrostatic potential), (b) the HOMOs, (where red indicates HOMOs with high electron density), (c) the LUMOs (where blue indicates LUMOs) and in (d) density of electrostatic potential on the molecular surface (where red indicates negative, blue indicates positive and green indicates neutral)

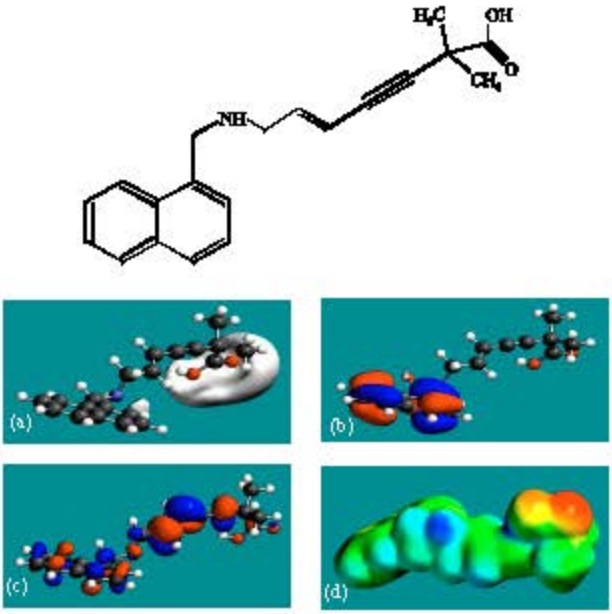

Fig. 11: Structure of CDTBN giving in: (a) the electrostatic potential (greyish envelope denotes negative electrostatic potential), (b) the HOMOs, (where red indicates HOMOs with high electron density), (c) the LUMOs (where blue indicates LUMOs) and in (d) density of electrostatic potential on the molecular surface (where red indicates negative, blue indicates positive and green indicates neutral)

In the case of TBN and DTBN, the electrostatic potential is found to be more negative around the amino nitrogen atom, around two fused aromatic rings and cylindrically around the two carbon atoms involved in C≡C bond, indicating that the positions may be subject to electrophilic attack. In the case of NAL, the electrostatic potential is found to be more negative around the carbonyl oxygen atom indicating that the positions may be subject to electrophilic attack. In the case of NM, the electrostatic potential is found to be more negative around the hydroxyl oxygen atom and around the two fused aromatic rings, indicating that the positions may be subject to electrophilic attack. In the case of NA, the electrostatic potential is found to be more negative around the carboxyl oxygen atoms, indicating that the positions may be subject to electrophilic attack. In the case of HTBN, the electrostatic potential is found to be more negative around the amino nitrogen atom, cylindrically around the two carbon atoms involved in C≡C bond and the hydroxyl oxygen atom, indicating that the positions may be subject to electrophilic attack. In the case of DATBN, the electrostatic potential is found to be more negative around the amino nitrogen atom, cylindrically around the two carbon atoms involved in C≡C bond and the carbonyl oxygen atom, indicating that the positions may be subject to electrophilic attack. In the case of CTBN and CDTBN, the electrostatic potential is found to be more negative around the amino nitrogen atom, hydroxyl and carbonyl oxygen atoms, once again indicating that the positions may be subject to electrophilic attack.

In the case of TBN, HTBN, DTBN and DHTBN, both HOMOs with high electron density and LUMOs are found to be centred mostly on the non-hydrogen atoms of the naphthalene moiety. In the case of NAL, NM and NA, both HOMOs with high electron density and LUMOs are found to be centred y on all the non-hydrogen atoms. In the case of TBN, HTBN, DTBN and DHTBN, both HOMOs with high electron density and LUMOs are found to be centred mostly on the non-hydrogen atoms of the naphthalene moiety. In the case of DATBN, CTBN and CDTBN HOMOs with high electron density are centred on the non-hydrogen atoms of the naphthalene moiety whereas LUMOs are centred on all or nearly all the non-hydrogen atoms. The overlap or close proximity of positions of HOMOs with high electron density and those of negative electrostatic potential give further support to the idea that the positions may be subject to electrophilic attacks.

TBN and its metabolites have solvation energy values ranging from -1.56 to -11.50 kcal $nmol^{-1}$ from PM3 calculations and dipole moments ranging from 0.6 to 5.2 from DFT calculations, indicating that the compounds would differ in their solubility in water. TBN is expected to be least soluble in water whereas the metabolite DCTBN would be most soluble.

When the surface area and volume of TBN are compared with those of its metabolites, it is found that the values for TBN (375.17 $Å^2$ and 352.63 $Å^3$ from DFT calculations) closely match with those of the toxic metabolite DATBN (377.84 $Å^2$ and 355.32 Å), suggesting that DATBN may also block the fungal squalene epoxidase.

When the densities of electrostatic potential on molecular surfaces (Fig. 2d-11d) are considered, it can be seen that the surfaces of all the compounds have neutral (green), electron-rich (red) and electron-deficient (blue) regions so that they may be subject to hydrophobic interaction and electrophilic and nucleophilic attacks. TBN, DATBN, NAL and DTBN are found to have more of electron-deficient regions so that they would be more likely to react with cellular nucleophiles such as glutathione and nucleobases in DNA. This means that the compounds would be most likely to cause depletion of cellular glutathione and oxidation of nucleobases in DNA. Depletion of glutathione would induce cellular toxicity by compromising the anti-oxidant status of the cell whereas oxidation of nucleobases in DNA would result into DNA damage. It may be noted that the metabolite DATBN that is found to most in electron-deficient regions, has been implicated as being the cause for toxicity of TBN.

CONCLUSIONS

Terbinafine (TBN) is an orally active allylamine derivative that has fungicidal activity against dermatocytes and many pathogenic fungi. The drug is extensively metabolized in humans with systemic clearance being dependent primarily on its biotransformation. Molecular modelling analyses based on molecular mechanics, semi-empirical and DFT calculations show that TBN and its metabolites have moderately large LUMO-HOMO energy differences, indicating that neither TBN nor any of its metabolites would be highly labile or extremely inert. The molecular surface of the metabolite DATBN that has been implicated as being the cause for toxicity of TBN is found to abound most in electron-deficient regions so that it may react most readily with cellular antioxidant glutathione and nucleobases in DNA. Reaction with reduced form of glutathione would cause its depletion resulting into oxidative stress and cellular toxicity whereas oxidation of nucleobases in DNA would cause DNA damage.

ACKNOWLEDGMENT

Fazlul Huq is grateful to the Discipline of Biomedical Science, The University of Sydney for the time release from teaching. Otherwise, it is not funded by any drug company.

REFERENCES

Baath, N.S., J. Hong and S.P. Sattar, 2006. Possible carbamazepine toxicity with terbinafine. Can. J. Clin. Pharmacol., 13: 228-231.

Humbert, C.H., M.D. Cabiac, J. Denouel and S. Kirkesseli, 1995. Pharmacokinetics of terbinafine and of its five metabolites in plasma and urine, following a single oral dose in healthy subjects. Biopharm. Drug Dispos., 16: 685-694.

Humbert, H., J. Denouel, M.D. Cabiac, H. Lakhdar and A. Sioufi, 1998. Pharmacokinetics of terbinafine and five known metabolites in children, after oral administration. Pharam. Drug Dispos., 19: 417-423.

Iverson, S.L. and J.P. Uetrecht, 2001. Identification of a reactive metabolite of terbinafine: Insights into terbinafine-induced hepatotoxicity. Chem. Res. Toxicol., 14: 175-181.

Ryder, N.S., 1989. The mechanism of action of terbinafine. Clin. Exp. Dermatol., 14: 110-113.

Spartan '02, 2002, Wavefunction, Inc., Irvine, CA, USA.

Vickers, A.E.M., Sinclair, M. Zollinger, F. Heitz, U. Glanzel, L. Johanson and V. Fischer, 1999. Multiple cytochrome P-450s involved in the metabolism of terbinafine suggest a limited potential for drug-drug interactions. Drug Metab. Dispos., 27: 1029-1038.